Synergistic effect of carbon nanofiber and sub-micro filamentary nickel nanostrand on the shape memory polymer nanocomposite

2011 Smart Mater. Struct. 20 035017

(http://iopscience.iop.org/0964-1726/20/3/035017)

Smart Mater. Struct. **20** (2011) 035017 (7pp) doi:10.1088/0964-1726/20/3/035017

Synergistic effect of carbon nanofiber and sub-micro filamentary nickel nanostrand on the shape memory polymer nanocomposite

Haibao Lu[1,2,3], **Jihua Gou**[2,3], **Jinsong Leng**[1,3] **and Shanyi Du**[1]

[1] National Key Laboratory of Science and Technology on Advanced Composites in Special Environments, Harbin Institute of Technology, Harbin 150080, People's Republic of China
[2] Department of Mechanical, Materials and Aerospace Engineering, University of Central Florida, Orlando, FL 32816, USA

E-mail: lhb1019@sohu.com, jgou@mail.ucf.edu and lengjs@hit.edu.cn

Received 12 October 2010, in final form 26 December 2010
Published 14 February 2011
Online at stacks.iop.org/SMS/20/035017

Abstract
This work studies the synergistic effect of carbon nanofiber (CNF) and sub-micro filamentary nickel nanostrand on the thermal and electrical properties, as well as the electro-active shape memory behavior, of a shape memory polymer (SMP) nanocomposite. The combination of electrical CNF and electromagnetic nickel nanostrand is used to render insulating thermo-responsive SMPs conductive. Subsequently, the shape memory behavior of the SMP can be activated by the electrical resistive heating. It is shown that sub-micro filamentary nickel-coated nanostrands significantly improved the electrical conductivity to facilitate the actuation of the SMP nanocomposite despite the low nanostrand volume content and low electrical voltage. Also the CNFs are blended with the SMP resin to facilitate the dispersion of nanostrands and improve the thermal conductivity to accelerate the electro- and thermo-active responses.

(Some figures in this article are in colour only in the electronic version)

1. Introduction

Thermo-responsive shape memory polymers (SMPs) are one of the shape memory materials that have the ability to change between shapes and demands [1]. They can undergo large deformation in the presence of temperature heating. This deformed shape can be kept when the stimulus is removed. Then, the SMPs are relaxed to their original shape after the stimulus is applied again. In comparison with shape memory alloys (SMA) and shape memory ceramics (SMC), SMPs have a number of intrinsic advantages including larger deformation strain, easier to manufacture, lower density, lower manufacturing cost and many more varieties in actuation approach [2–4]. These unique characteristics enable the SMP to be used in a myriad of fields, including clothing manufacturing, automobile engineering, aerospace engineering, medical treatment and many other applications [1, 5]. With the application domain of SMPs growing, some major limitations of SMPs still exist and impose major challenges to their broad utilization [6]. Some of the key limitations include low recovery force due to low rubbery moduli, low recovery speed due to the low thermal conductivity and inertness to electromagnetic stimuli (in contrast to SMAs), owing to the electrical insulation of most polymeric materials. Fortunately, many interesting and valuable research efforts have begun to address these challenges. With regard to the last challenge listed above, a variety in the actuation approach for SMPs has been developed. Currently, the shape recovery can not only be induced by external stimuli such as temperature heating, but also can be manipulated by light [2], infrared light-heating [7], water [8], solvent [9–12], magnetic field [13, 14] or electrically

[3] Authors to whom any correspondence should be addressed.

resistive Joule heating [15–21]. For the actuation of SMP composites (fabricated by filling the conductive filler into the SMP) induced by electrically resistive heating, the conductive filler generates heat according to Joule's law and eventually facilitates the heat transfer to trigger shape recovery. However, the electrical conductivity of electro-active material systems is still relatively low, due to the limited efficiency of discrete fillers to form percolating conductive networks. In addition, the electrical conductivity of fillers is not that high until the sub-micro filamentary nickel nanostrand was found.

The revolution in nanotechnology has resulted in a wide variety of nanostructured materials in many formats, such as films, spheres, tubes and filaments [22, 23]. Many metals and alloys are available in nanostructured formats, such as powders or crystals. Recently, filamentary metals have been available and are known as 'nanostrands'™. Nanostrands have many potential applications. Being metal, they provide excellent mechanical nanoreinforcement. Being magnetic, they also provide some unique nanomagnetic properties. These contemplated multi-functions can serve to solve multiple problems. Normally non-conductive materials have been rendered partially conductive by the addition of electrically conductive fillers. Most of these commercial additive solutions are based on the elements copper, silver, nickel or carbon, in the physical forms of particles, fibers or films. Meanwhile the normally lower aspect ratio of these materials necessitates higher added fractions. In contrast, a higher aspect ratio would result in a lower added fraction saving, largely due to that the nanostrands could be created as a very porous three-dimensional lattice of interconnected strands.

Thus far, the merits of nickel nanostrands have been extolled. It provides an attractive solution to many conductive polymer problems. However, it would provide a broad spectrum of solutions if it was used in combination with carbon nanofibers (CNF). The advantage of adding nickel nanostrands to a conductive CNF composite system is that it only requires a small amount of nanostrands to create conductive paths from nanofiber to nanofiber and throughout the polymer. In addition, the nanostrands tend to fill in the previously resin-rich areas of the polymer, so that even these regions become conductive. On the other hand, another advantage of adding both CNFs and nickel nanostrands is that both phases of the composite are conductive and the added margin of conductivity is often accompanied by multi-functional attributes that characterize these combinations of materials. Against this background, a unique concept of making nanocomposites from CNFs and nickel nanostrands has been explored. The synergistic effect of CNFs and nickel nanostrands on the electrical properties, and electro- and thermo-active behavior of SMP nanocomposites will be considered in this study.

SMPs are smart materials with potential applications as, for example, actuators [19], self-adjusting orthodontic wires and selectively pliable tools for small-scale surgical procedures. Another application of SMPs in the medical field could be their use in implants: for example, minimally invasive, through small incisions or natural orifices, implantation of a device in its small temporary shape. Shape memory technologies have shown great promise for cardiovascular stents, since they allow a small stent to be inserted along a vein or artery and then expanded to prop it open [24]. Further potential applications include morphing aircraft and deployable structures. SMPs may also be useful in the production of aircraft which would morph during flight. Currently, the Defense Advanced Research Projects Agency (DARPA) is testing wings which would change shape by 150% [25]. Moreover, a hinge made of SMP and carbon fiber has been fabricated and a prototype of a solar array actuated by the SMP composite hinge has been successfully deployed [26].

2. Experimental details

CNFs (Pyrograf®-III, PR-HHT-25) are supported by Applied Sciences Inc., Cedarville, OH, USA. They were further treated at a temperature of 2200 °C to obtain a complete graphitic structure and purified to a very high level (>99 wt%). Such heat treatment could also help to reduce the iron catalyst content to a very low level (<0.8 wt%). The nanofibers have diameters of 50–100 nm and lengths of 30–100 μm. The CNFs were dispersed into distilled water with a non-ionic surfactant $C_{14}H_{22}O(C_2H_4O)_n$ (Triton X-100, supplied from BYK-Chemie USA, Inc, Wallingford, CT, USA). Also the non-ionic surfactant was added to aid the dispersion of CNFs in water. The suspension was sonicated with a high-intensity sonicator (MISONIX Sonicator 4000, Qsonica, LLC, Newtown, CT, USA) at room temperature for 30 min. Finally, the CNF suspension was then filtered through a 0.4 μm hydrophilic polycarbonate membrane under high pressure and dried in an oven at 120 °C for 2 h to remove the remaining water and surfactant.

The nickel nanostrands are supplied from Conductive Composites Company LLC, Midway, UT, US. This nanostrand is grown by the low temperature atmospheric pressure chemical vapor decomposition process (LTAPCVD). The strands initially grow as a three-dimensional self-supporting lattice of interconnected filaments. The as-grown lattice is about 99.8% porous. Nanostrands are self-assembled three-dimensionally branched and interconnected high aspect ratio sub-micro chains of neat nickel. They form a volumetrically continuous network of nano- and micro-level Faraday cages. The have a highly uniform, smooth, conformal and ductile coating with controlled thickness between 20 and 2000 nm. The nanostrands do not take much energy to disperse them into most resins due to the fact that too much energy will shear the strands apart and reduce them to particulate powder. Low shear and low viscosity methods have shown the most success for dispersing nanostrands. In this study, the nanostrands are dispersed into distilled water (with a ratio of 1 g:100 ml) and heated at a temperature of 150 °C at 10 °C min^{-1} until the water has volatilized completely. This treatment will help the as-received nanostrands to reach its nanosize.

The epoxy SMP (Veriflex® E2,) is a product of Cornerstone Research Group (CRG) Inc., Dayton, OH, USA. The Veriflex E2 is a fully formable, thermoset, SMP resin system. This system contains two components (called part A and part B). Part A will be cured with part B at a weight ratio of 100 g:27.05 g. The resulting mixture was mechanically stirring

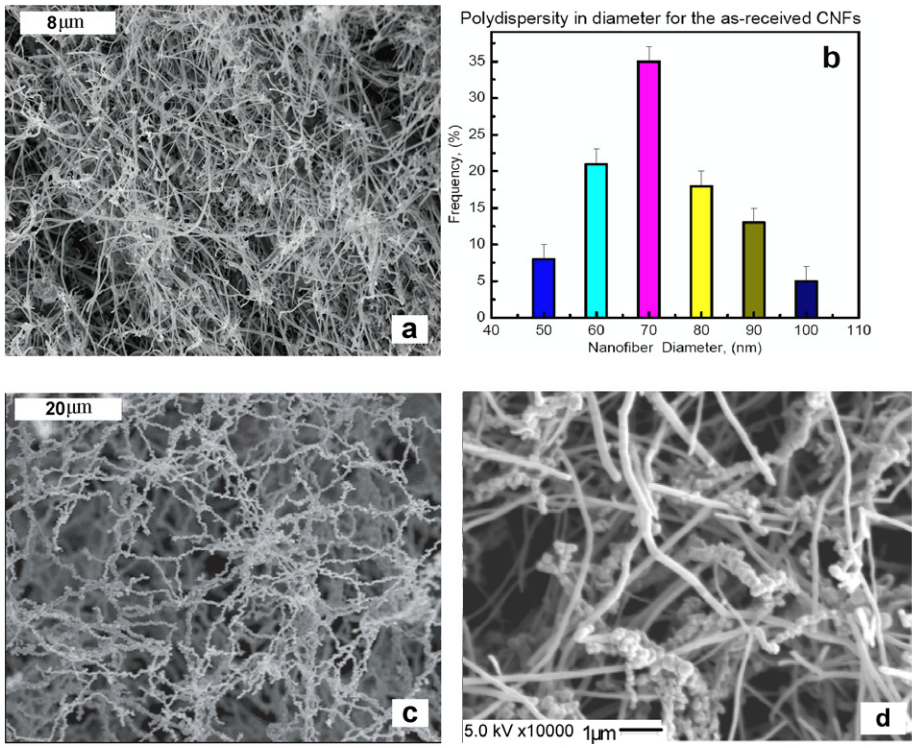

Figure 1. (a) Morphologies and network structure of CNFs (at a magnification of 3000×). (b) The histograms of nanofiber diameters (observed by image analysis) for the as-received nanofiber sample. (c) Morphologies and network structure of nickel nanostrands (at a magnification of 10 000×), copyright reserved from Society for the Advancement of Material and Process Engineering. (d) Morphologies and network structure of hybrid mixture making of nickel nanostrands and CNFs,

with a high shear mixer. The cured Veriflex E2 combines shape memory properties with high mechanical stiffness and strength. Also it is capable of regaining its original shape on nearing 103 °C. Then, the as-treated CNFs and nanostrands were blended into the polymer matrix at a proper ratio. The mixture was degasified in a vacuum oven to completely remove the air bubbles at room temperature for 40–90 min. Finally, the matrix was then injected into a mold and cured in a convection oven from room temperature to 130 °C at 5 °C min^{-1}, followed by an isothermal hold for 6 h under air environment. Also it needs to be post-cured without dimensional constraint at 150 °C for 2 h.

In this study, five types of SMP nanocomposites were prepared, including pure SMP, an SMP nanocomposite filled with 2.5 wt% CNFs, an SMP nanocomposite filled with 2.5 wt% CNFs and 2.5 wt% nanostrands, an SMP nanocomposite filled with 2.5 wt% CNF and 5 wt% nanostrands, as well as an SMP nanocomposite filled with 2.5 wt% CNFs and 7.5 wt% nanostrands.

3. Results and discussion

3.1. Morphology and structure of CNF and nanostrand

The morphology and structure of the CNF were characterized using scanning electron microscopy (SEM, ZIESS Ultra-55) at an accelerating voltage of 5 keV and magnification of 3000×. Figure 1(a) is a typical surface view of the raw CNF arrays. The CNFs have diameters ranging from 50 to 100 nm and are entangled with each other. A network structure was formed by the molecular interaction and mechanical interlocking between individual nanofibers. Figure 1(b) shows the histograms of nanofiber diameters (observed by image analysis) for the as-received nanofiber sample. It is noted that the average nanofiber diameter ranged from 45 ± 2 to 105 ± 2 nm. The polydispersity in nanofiber diameters shows a normal distribution trend. According to figure 1(c), the nanostrand is approximately 50–500 nm in diameter and tens to hundreds of microns long. This characteristic results in the nanostrand having a high aspect ratio. The nanostrand has a very porous three-dimensional lattice of interconnected strands, with strands entangled with each other and mechanical interlocking. Such a continuous network would provide conductive paths for electrons as an electrical current is applied. As shown in figure 1(d), this micrograph presents a hybrid mixture of nickel nanostrands and CNFs. These nanofibers and nanostrands are entangled with each other. A network structure was formed by the molecular interaction and mechanical interlocking among individual nanofibers and nanostrands. These interconnected nanofibers and nanostrands would create conductive paths throughout the resin for electrons. As a result, the co-supporting two-filler is expected to enhance conductivity and therefore synergistic effects are expected.

3.2. Electrical resistivity measurement

The electrical resistivity of the pure SMP and SMP nanocomposites were first measured by a standard four-probe system (SIGNATONE QUADPRO) incorporated with a precision multimeter. The apparatus has four probes in a straight line with an equal inter-probe spacing of 1.56 mm. The radius of the probe needle is 100 μm. A constant current passes through two outer probes and an output voltage is measured across the inner probes with the voltmeter. The electrical resistance was calculated as

$$R_s = 4.53 \times \frac{V}{I} \tag{1}$$

where R_s is the electrical resistance, V is the voltage applied on the outer two probes and I is the electrical current passed through the inner two probes.

Furthermore, the electrical resistivity (ρ) and conductivity (σ) were calculated as

$$\rho = R_s \frac{A}{l} \qquad \text{and} \qquad \sigma = \frac{1}{\rho} \tag{2}$$

where A and l are the cross-sectional area and distance between two electrodes, respectively.

The electrical resistivity of the SMP samples was plotted against various concentrations of conductive filler, as shown in figure 2. For all four SMP nanocomposite samples with the same concentration of conductive filler, there is a difference in electrical resistivity owing to the inhomogeneous dispersion of hybrid filler in the nanocomposite. The error bars shown in the figures represent standard deviations. This is indicative of the appreciable variability in electrical resistivity of the tested samples. As the concentration of hybrid filler increases from 0 to 10.0 wt%, the average electrical resistivity of the tested samples is reduced from 10.00^{14}, 12 536.36, 226.47, 31.02 to 1.78 Ω cm. As previously mentioned, a synergetic effect resulting in a reduction of the low resistivity of the nanocomposite is expected. In comparison, the volume resistivity of the nanocomposite filled with 2.5 wt% CNFs, is nearly 6000 times higher than that filled with 2.5 wt% CNFs and 7.5 wt% nanostrands. This can be attributed to the fact of the inherent superconductive property, high aspect ratio and orientation of nickel nanostrands. At the same time, the CNF also has a high aspect ratio and excellent electrical properties. Therefore, synergistic effect of CNFs and nanostrands makes them form a three-dimensional network in the nanocomposites. The more hybrid filler involved, the more conductive paths are formed. Given more conductive CNFs and nanostrands in one bulk, the current-carrying capability and electrical current amplitude increase because more electrons are forced to pass through the cross section of the bulk. In addition, more hybrid fillers are going to increase the probability of forming relative shorter distances for the electron flow and making the period time of electron flow shorter. These three approaches would significantly decrease the electrical resistivity of SMP nanocomposites.

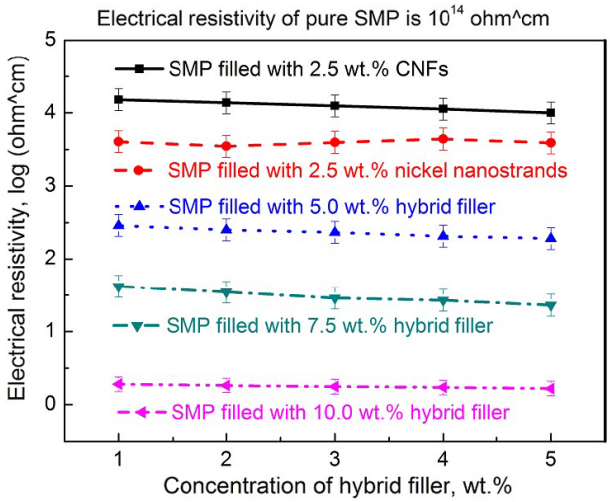

Figure 2. Electrical resistivity of SMP matrix and its nanocomposites as a function of the concentration of hybrid filler.

3.3. Effect of hybrid filler on the T_g of nanocomposites

The shape memory effect of epoxy-based SMPs functions on the thermal activation customizable by the T_g. The study on T_g is a basic approach to characterize the shape memory behavior of SMPs and their nanocomposites.

Differential scanning calorimetry (DSC) is a technique in which the difference in energy inputs into a substance (and/or its reaction product(s)) and a reference material is measured as a function of temperature whilst the substance and reference material are subjected to a controlled temperature program. We use it to study the thermal transitions of a polymer, where these thermal transitions take place in a polymer when it is heated. The glass transition is a thermal transition. Here, the T_g of the SMP samples will be determined with this method. DSC experiments were conducted on a Netzsch (Selb, Germany) DSC 204F1 instrument. All experiments were performed with a constant heating and cooling rate of 10 °C min^{-1}. The samples were investigated in the temperature range from 10 to 120 °C. The sample was heated from 10 to 120 °C, then cooled down to 10 °C, and again warmed up to 120 °C. Whenever a maximum or minimum temperature in the testing program was reached, this temperature was kept constant for 2 min. The T_g was determined from the second heating run. Experimental results reveal that the nickel nanostrands have a negative effect on the T_g of SMP nanocomposite samples, and with an increase in filler concentration the reduction in T_g becomes greater. As presented in figure 3, T_g is determined as 64.932, 71.172, 60.276, 59.414 and 58.310 °C for pure SMP, SMP nanocomposite with 2.5 wt% CNFs, SMP nanocomposite with 5.0 wt% hybrid filler, SMP nanocomposite with 7.5 wt% hybrid filler and SMP nanocomposite with 10.0 wt% hybrid filler, respectively. As is known, a chemically cross-linked structure was formed by macromolecular chains during the curing process of the thermosetting SMP resin. The relative motion of macromolecule segments or chains is the primary mechanism of the shape memory effect. Therefore, the change in T_g of SMP nanocomposites should be attributed to

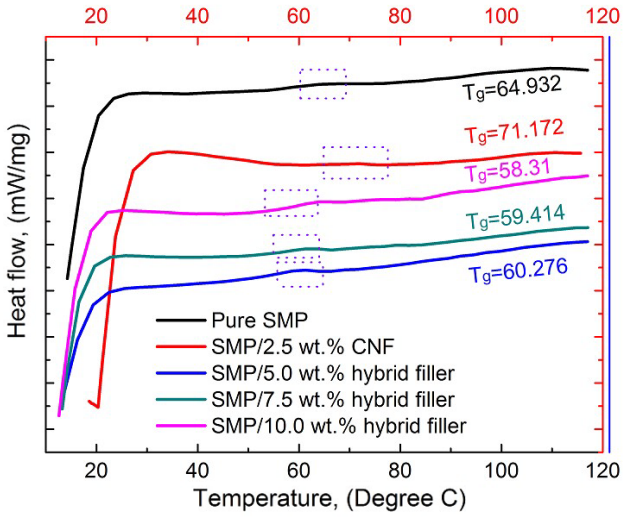

Figure 3. DSC results of SMPs with various concentrations of conductive filler.

the influence of the filler on the motion of macromolecule segments. The as-received CNFs have a characteristic size of 50–100 nm, which is of the same order as the size of a typical segment, approximately 10–1000 nm. At the same time, the CNFs have a stronger interaction with the macromolecules and the motion of macromolecules will be prevented by the CNFs, resulting in the macromolecules requiring more heat energy from an external source to overcome the friction among macromolecules and nanofibers. Here, the T_g of an SMP nanocomposite filled with CNFs is therefore enhanced. On the other hand, the density of nickel nanostrands is higher than the polymer resin, and they have no active groups reacting with the resin to form a strong or stable bonding. Therefore, the nickel nanostrands only prevent close packing of the macromolecules. The thermal stability of SMP nanocomposites would be reduced by an increase in the content of nickel nanostrands. As a result, the T_g of the SMP nanocomposite was gradually depressed. Also the more dramatic decrease in T_g in the presence of nickel nanostrands can be attributed to the particle's density and interfacial characterization.

3.4. Synergistic effect of hybrid filler on the actuation of SMPs

The function and effectiveness of the hybrid filler in the actuation of the SMP by electrically resistive heating were experimentally conducted using a '∏'-shaped geometry and a DC power supply. Digital images were taken using an infrared camera (VarioCAM) and with the sample imaged from the size necessary to visualize the sample curvature.

Figure 4 records the shape recovery of the SMP nanocomposite filled with 2.5 wt% CNFs and 7.5 wt% nanostrands. The flat (permanent shape) SMP sample with a dimension of 90 mm × 7.5 mm × 1.0 mm was bent into a 'U'-like shape (temporary shape) at 150 °C. This shape was kept until the specimen was cooled down to room temperature. No apparent shape recovery was found after the deformed specimen was kept in air for 2 h. A constant 36 V direct current voltage was applied to the sample, where there was a constant 0.03 A electrical current flowing through it. The SMP nanocomposite took 60 s to complete the shape recovery from the bent shape. Initially the nanocomposite showed a small recovery ratio during the first 10 s. It then started to exhibit a faster recovery behavior until 60 s. Finally, the nanocomposite did not show a 100% recovery ratio as it did not completely return to its initially flat shape. This small absence of complete shape recovery ratio could be attributed to the interface friction among the CNFs, nanostrands and the polymer molecules. In addition, the SMP part may lack enough mechanical strength at the switching temperature to pull on the hybrid filler to return to its original shape. Furthermore, it should be noted that the rate of shape recovery was strongly dependent on the magnitude of the applied electric power and the electrical properties of the nanocomposite.

3.5. Thermally responsive shape memory behavior

The synergistic effect of CNFs and nanostrands on the electro-active shape recovery of SMP nanocomposites has been found and the actuation by electrical resistive heating has been achieved. The combination of conductive CNFs and nanostrands was also used to improve the thermal conductivity to facilitate the heat transfer and absorption of the SMP nanocomposite.

Thermally responsive SMP materials had been endowed with electrically conductive properties by introducing CNFs and nanostrands. However, the SMP nanocomposite incorporated with different concentrations of hybrid filler will have a distinct response behavior to the thermal stimuli. Also it should be noted that the difference in behavior also results from the thermal conductivity of various SMP samples. The thermal conductivity of pure SMP is 0.17 W K^{-1} m^{-1}, where the thermal conductivity of SMP nanocomposites is ranged from 0.5 to 2.0 W K^{-1} m^{-1} as the concentration of conductive filler increased from 2.5 to 10.0 wt%. The thermally responsive behavior of pure SMP and its nanocomposites was evaluated by shape recovery angle with respect to shape recovery time. The isothermal shape recovery experiments of samples with rectangular geometry of constant dimensions 70 mm × 10 mm × 3.5 mm were conducted. The sample was first heated above its switching temperature, quickly deformed by hand into a bent shape and allowed to cool to room temperature for shape fixing. The recovery ratio was calculated based on the change of deformation angle during recovery. The recovery ratio, R, is defined as [6]

$$R(\%) = \frac{\theta_i - \theta(t)}{\theta_i - \theta_e} \tag{3}$$

where θ_i, $\theta(t)$ and θ_e are the initial deformation angle of the fixed sample, the deformation angle at a given time t and the deformation angle at the equilibrium state (in our case $\theta_e = 0$), respectively. The shape recovery was triggered by immersing the deformed samples into an infrared oven at 130 °C. The resulting recovery profiles are shown in figure 5(a). From these curves, they reveal that the SMP sample with 10.0 wt% hybrid filler has the fastest response behavior to the thermal stimulus

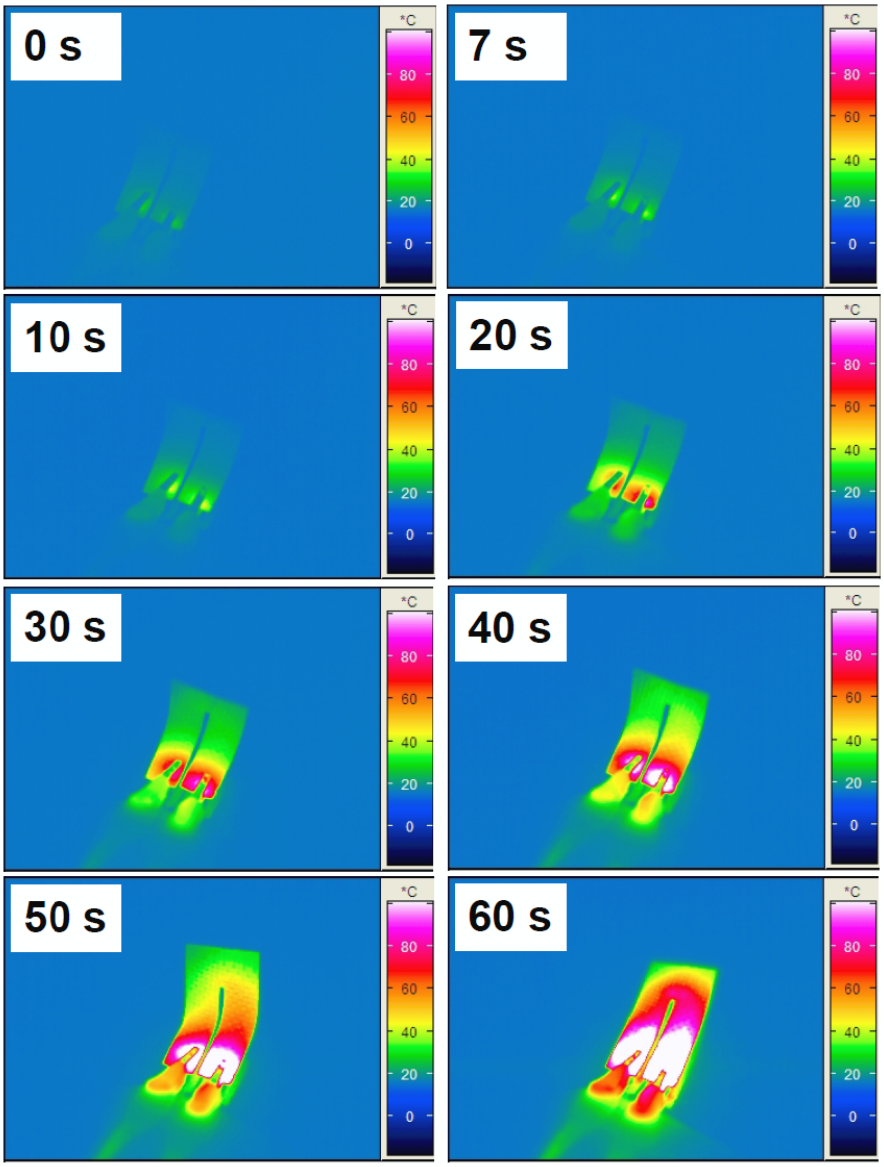

Figure 4. Time-resolved photographs showing the electro-active shape memory effect and temperature distribution of SMP nanocomposites integrated with 2.5 wt% CNFs and 7.5 wt% nanostrands, under a constant DC voltage of 36 V. The permanent shape is a flat strip of nanocomposite material and the temporary shape is deformed as a right-angled shape.

(it completes the shape recovery in 313 s). Otherwise the pure SMP sample has the slowest response behavior to the thermal stimulus, where it completes the shape recovery within 407 s. The recovery ratios of all the samples are approximately 98%.

To reveal more detailed kinetics information, the recovery data were further analyzed using a standard Boltzmann function [6]:

$$R(t) = A_2 + \frac{A_1 - A_2}{1 + \mathrm{e}^{(t-t_0)/\tau}} \tag{4}$$

where A_1, A_2, t_0 and τ are the four fitting parameters. Each fitting curve reveals a Boltzmann equation. Also all the four fitting parameters can be obtained from the experimental results. So, the dataset for each curve is $A_1 = -1.294\,04$, $A_2 = 99.0664$, $t_0 = 250.830\,46$ and $\tau = 40.925\,37$, $A_1 = -0.750\,06$, $A_2 = 103.161\,23$, $t_0 = 235.063\,26$ and $\tau = 36.223\,69$, $A_1 = 0.011\,17$, $A_2 = 103.549\,57$, $t_0 = 219.647\,49$ and $\tau = 31.091\,69$, $A_1 = -0.182\,67$, $A_2 = 107.433\,54$, $t_0 = 218.751\,65$ and $\tau = 31.879\,22$ and $A_1 = 0.132\,35$, $A_2 = 111.115\,47$, $t_0 = 217.676\,57$ and $\tau = 32.484\,01$, respectively. The fitted curves have R^2 values of 0.998 16, 0.9992, 0.998 27, 0.9997 and 0.992 21, respectively, and are shown as solid lines in figure 5(a). The second derivatives of the fitted curves were then calculated and plotted in figure 5(b). All the second derivative plots show a similar pattern consisting of two opposite peaks with the same height. The induction time is defined as the time between 0 (when the voltage was applied) and the first (positive) peak on the second derivative plot. This corresponds to an induction period of the recovery profile shown in figure 5(b), during which the sample was heated from the environmental temperature to its switching temperature. In

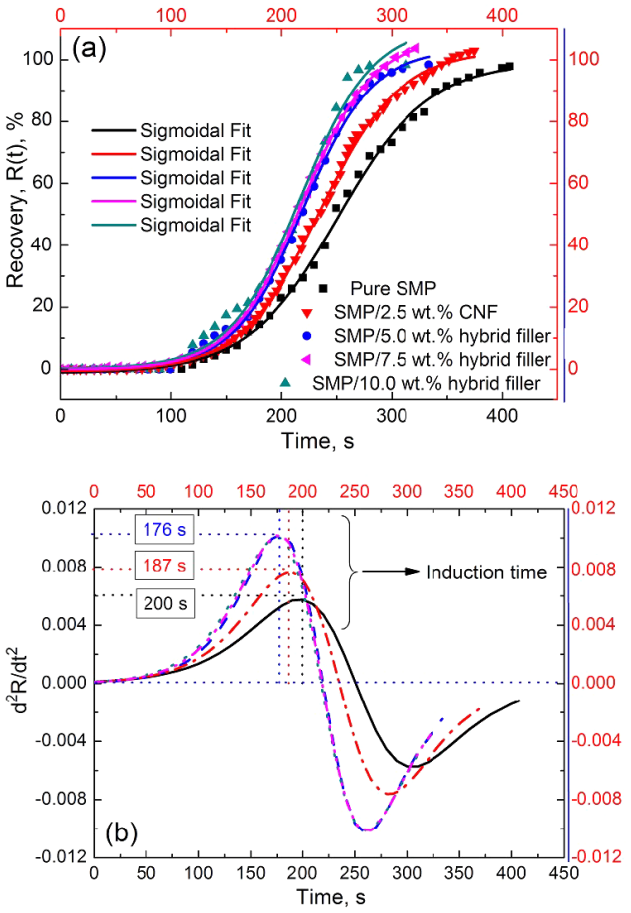

Figure 5. (a) Thermally activated shape recovery of SMP/CNF/nanostrand nanocomposites. (b) Three characteristic times were defined using the second derivative plots of the fitted Boltzmann function.

comparison with these three curves, it is found that the pure SMP sample has the longest induction time of 253 s, while the SMP nanocomposite filled with 10.0 wt% hybrid filler has the shortest induction time of 219 s.

Therefore, the hybrid filler has a positive effect on the responsive behavior of SMP to the thermal stimulus, resulting in the recovery time and induction time of SMP nanocomposites being reduced. This tendency increases with an increase in the concentration of hybrid filler. This experimental result demonstrates that the thermal conductivity of SMP nanocomposites has been significantly improved.

4. Concluding remarks

To conclude, a unique SMP nanocomposite with unprecedented electrical actuation capability has been developed by incorporating conductive CNFs and nanostrands into an epoxy-based SMP matrix. Besides the excellent electrical conductivity, this hybrid filler simultaneously enhances the thermal conductivity of the SMP. Multi-functional shape memory materials utilizing this exciting material are expected to be designed in our lab, owing to its improved thermally, electrically and magnetically responsive shape recovery behavior. Even though SMP actuation progresses rapidly, numerous challenges still remain in SMP development such as the increase in recovery force, stiffness and strength, acceleration of recovery time, etc. Among the major challenges, the durability of electrical SMP composites is an important facet and should therefore deserve more attention in the future. Continued research in mechanics modeling is needed, particularly research focusing on accurate modeling of time-dependent and finite-strain shape memory phenomena.

References

[1] Leng J S, Lu H B, Huang W M, Liu Y J and Du S Y 2009 *MRS Bull.* **34** 848–55
[2] Lendlein A, Jiang H, Junger O and Langer R 2005 *Nature* **434** 879–82
[3] Bellin I, Kelch S, Langer R and Lendlein A 2006 *Proc. Natl Acad. Sci. USA* **103** 18043–7
[4] Lendlein A and Kelch S 2002 *Angew. Chem. Int. Edn* **41** 2034–57
[5] Meng Q H and Hu J L 2009 *Composites* A **40** 1661–72
[6] Luo X F and Mather P T 2010 *Soft Matter* **6** 2146–9
[7] Leng J S, Wu X L and Liu Y J 2009 *J. Appl. Polym. Sci.* **30** 1–11
[8] Huang W M, Yang B, An L, Li C and Chan Y S 2005 *Appl. Phys. Lett.* **86** 114105
[9] Leng J S, Lv H B, Liu Y J and Du S Y 2008 *Appl. Phys. Lett.* **92** 206105
[10] Lu H B, Leng J S, Liu Y J and Du S Y 2009 *Smart Mater. Struct.* **18** 085003
[11] Lv H B, Leng J S, Liu Y J and Du S Y 2008 *Adv. Eng. Mater.* **10** 592–5
[12] Lu H B, Liu Y J, Leng J S and Du S Y 2010 *Eur. Polym. J.* **46** 1908–14
[13] Schmidt A M 2006 *Macromol. Rapid Commun.* **27** 1168–72
[14] Buckley P R, McKinley G H, Wilson T S, Small W IV, Benett W J, Bearinger J P, McElfresh M W and Maitland D J 2006 *IEEE Trans. Bio-Med. Eng.* **53** 2075–83
[15] Leng J S, Lv H B, Liu Y J and Du S Y 2007 *Appl. Phys. Lett.* **91** 144105
[16] Leng J S, Lv H B, Liu Y J and Du S Y 2008 *J. Appl. Phys.* **104** 104917
[17] Liu Y J, Lv H B, Lan X, Leng J S and Du S Y 2009 *Compos. Sci. Technol.* **69** 2064–8
[18] Lu H B, Liu Y J, Gou J H, Leng J S and Du S Y 2010 *Appl. Phys. Lett.* **96** 084102
[19] Lu H B, Yu K, Liu Y J and Leng J S 2010 *Smart Mater. Struct.* **19** 065014
[20] Lu H B, Yu K, Sun S H, Liu Y J and Leng J S 2010 *Polym. Int.* **59** 766–71
[21] Lu H B, Liu Y J, Gou J H, Leng J S and Du S Y 2010 *Smart Mater. Struct.* **19** 075021
[22] George H 2005 *SAMPE J.* **41** 1–11
[23] Low T 2002 *Adv. Mater. Process.* **160** 62–5
[24] Christopher M Y, Robin S, Craig L, Bryan R, Alex E and Ken G 2007 *Biomaterials* **28** 2255–63
[25] Sofla A Y N, Meguid S A, Tan K T and Yeo W K 2010 *Mater. Des.* **31** 1284–92
[26] Lan X, Liu Y J, Lv H B, Wang X H, Leng J S and Du S Y 2009 *Smart Mater. Struct.* **18** 024002